# Integrating a hydrogen fuel cell electric vehicle with vehicle-to-grid technology, photovoltaic power and a residential building

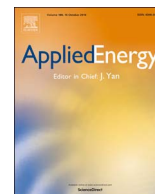Robledo, Carla B.; Oldenbroek, Vincent; Abbruzzese, Francesca; van Wijk, Ad J.M.

**Important note**
To cite this publication, please use the final published version (if applicable).
Please check the document version above.

# Integrating a hydrogen fuel cell electric vehicle with vehicle-to-grid technology, photovoltaic power and a residential building

Carla B. Robledo*, Vincent Oldenbroek, Francesca Abbruzzese, Ad J.M. van Wijk

*Energy Technology Section, Department of Process and Energy, Delft University of Technology, Leeghwaterstraat 39, 2628 CB Delft, The Netherlands*

## HIGHLIGHTS

- First time vehicle-to-grid measurements with a hydrogen fuel cell electric vehicle.
- Case study based on a Dutch pilot project.
- 2-week pilot living experiment in an all-electric house and using FCEV2G power.
- 52 h and 9 h of interrupted V2G at 1 kW and 10 kW power output, respectively.
- FCEVs can integrate transport and electricity sectors in a sustainable energy system.

## GRAPHICAL ABSTRACT
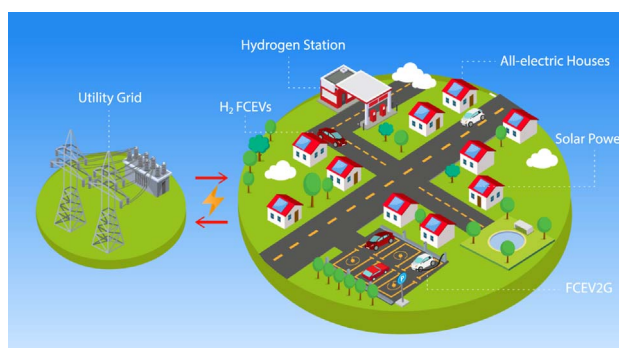


## ARTICLE INFO

## ABSTRACT

This paper presents the results of a demonstration project, including building-integrated photovoltaic (BIPV) solar panels, a residential building and a hydrogen fuel cell electric vehicle (FCEV) for combined mobility and power generation, aiming to achieve a net zero-energy residential building target. The experiment was conducted as part of the Car as Power Plant project at The Green Village in the Netherlands. The main objective was to assess the end-user's potential of implementing FCEVs in vehicle-to-grid operation (FCEV2G) to act as a local energy source. FCEV2G field test performance with a Hyundai ix35 FCEV are presented. The car was adapted using a power output socket capable of delivering up to 10 kW direct current (DC) to the alternating current (AC) national grid when parked, *via* an off-board (grid-tie) inverter. A Tank-To-AC-Grid efficiency (analogous to Tank-To-Wheel efficiency when driving) of 44% (measured on a Higher Heating Value basis) was obtained when the car was operating in vehicle-to-grid (V2G) mode at the maximum power output. By collecting and analysing real data on the FCEV power production in V2G mode, and on BIPV production and household consumption, two different operating modes for the FCEV offering balanced services to a residential microgrid were identified, namely fixed power output and load following.

Based on the data collected, one-year simulations of a microgrid consisting of 10 all-electric dwellings and 5 cars with the different FCEV2G modes of operation were performed. Simulation results were evaluated on the factors of autonomy, self-consumption of locally produced energy and net-energy consumption by implementing different energy indicators. The results show that utilizing an FCEV working in V2G mode can reduce the annual imported electricity from the grid by approximately 71% over one year, and aiding the buildings in the microgrid to achieve a net zero-energy building target. Furthermore, the simulation results show that utilizing the

FCEV2G setup in both modes analysed, could be economically beneficial for the end-user if hydrogen prices at the pump fall below 8.24 €/kg.

## 1. Introduction

Wind and solar photovoltaics are currently the fastest growing sources of electricity globally. Electricity generation from both technologies is constrained by the varying availability of wind and sunshine, which causes fluctuations in electricity output over time [1]. Their integration into current power systems, combined with the increased environmental and security concerns regarding energy supply is leading to a profound transformation in the current fossil-fuel based energy system. Distributed energy sources and energy storage are both becoming key components in this new system. The evolutionary trend of this transition is towards smart energy networks that are characterized by widespread deployment of renewable energy technologies and intelligent energy management systems [2]. Until now, the electricity system has developed independently from other energy-related systems. The recent trend seeks the integration of the electricity, heat and transport sectors in order to conceive a single energy system, or what is known as a Smart Energy System, Smart Urban Energy Network or Smart Cities [2–4]. Integrating power, heat and fuel networks can increase the utilization of the system, reduce total costs and offer national electricity systems greater flexibility [5].

While Smart Energy Systems are explored on a global level, Smart Grids are the basic underlying unit on the local level. Different energy products and services that are involved in Smart Grids include micro-generators, storage systems, smart appliances, time variable prices and contracts, and energy monitoring and control systems [6]. All of these are bound to or located near buildings; thus, in this framework, the integration of buildings into smart grids is fundamental [7]. On average most people in the developed world currently spend 90% of their lives indoors [8–10], relying on heating and air conditioning. This leads to buildings being the largest energy consumers worldwide, accounting for about 40% of global energy and approximately one-third of greenhouse gas (GHG) emissions [11].

In addition, most road transport energy consumption is due to passenger vehicles, and when they are not in use, they are usually parked close to buildings [12]. Significant energy and environmental savings could be achieved if buildings were designed and managed efficiently and passenger vehicles were integrated into the built environment. It is estimated that an energy demand reduction of 35% can be achieved for a household by incorporating thermal insulating layers, utilizing energy-efficient appliances, efficient illumination and changing from fossil-fuel based to electric cars. However, this reduction in total energy is directly connected to an increase in electricity demand of 150% [13]. For the system to be sustainable, all of these 'all-electric' households will have to be supplied with electricity from renewable sources, such as solar and wind.

The conceptual understanding of a zero-energy building (ZEB) is that it is an energy-efficient building able to generate electricity, or other energy carriers, from renewable sources in order to compensate for its energy demand. More specifically, the term *near or net* ZEB (NZEB) is used to refer to buildings that are connected to the energy infrastructure, underlining the fact that there is balance near or equal to zero between energy taken from and supplied back to the energy grid over a period of time, nominally one year [14]. The end-users living in these buildings are sometimes referred to as 'prosumers', as they not only consume energy but also produce it on-site. The term often describes consumers who rely on smart meters and solar PV panels to generate electricity and/or combine these with home-energy management systems, energy storage, electric vehicles (EVs) and vehicle-to-grid (V2G) systems [15].

In this framework, electric vehicles become a fundamental component of buildings. The great potential in reducing energy demand in the built environment is reflected globally in policy directions that are moving towards zero-energy standards [16]. For example, the European Union (EU) has established that by 2021, all new buildings must be close to ZEB, and by 2019, new buildings occupied and owned by public authorities must also be close to ZEB [17]. While in California in the United States, the California Public Utilities Commission adopted the Big Bold Initiative, which directed that all new residential and commercial construction be Zero Net Energy by 2020 and 2030, respectively [18]. The technical feasibility of such zero-energy buildings has been proven by several pilot and case studies [19]. Some of them have even proven the ability of residential buildings to become positive-energy buildings (PEB), producing more energy than they consume [20,21].

Both intraday and seasonal energy storage systems are needed to support the integration of renewable energy. Typical solutions include electrical energy storage in batteries, flywheels, compressed air energy storage, pumped storage, EVs and hydrogen as an energy carrier [22–24]. While batteries will be used for short-term energy-efficient storage, long-term (seasonal) storage will require hydrogen fuels [25]. Energy storage, in the form of hydrogen and its direct use in fuel cells, can ensure reliability to the energy system and assist in the integration of renewable energy supply into the residential and industrial sectors. Electricity, heat and water are produced when hydrogen reacts with oxygen in a fuel cell. Hydrogen can be used in the transport sector in fuel cell electric vehicles (FCEVs). It is also important to mention the positive environmental effect caused by the replacement of gasoline vehicles by FCEVs. It has recently been reported by Ahmadi et al. that a 72% reduction in total GHG emissions (in terms of $gCO_2$ equivalent emitted per km of vehicle travelled) can be obtained by switching from gasoline vehicles to FCEVs in the transportation sector and that they are becoming both technologically and economically viable compared with incumbent vehicles [26].

In a recent review, Alanne and Cao defined the concept of the 'zero-energy hydrogen economy' as a zero-energy system, where hydrogen is one of the key energy carriers [27]. The review focuses on the integration of zero-energy hydrogen vehicles at the level of single buildings and communities and suggests that more research is needed to understand the impact of the exchange of various energy types between these vehicles, buildings and/or communities and hybrid smart grids. In this study, we aim to bridge this knowledge gap by providing insight into the technical feasibility of integrating a fuel cell electric vehicle with a residential building of a prosumer type, in order to fulfil the zero-energy building target.

EVs are considered promising candidates to replace fossil fuel powered vehicles. They not only have the potential to yield cleaner transportation but can also provide electric storage capabilities for other applications, such as V2G, Vehicle-to-Home (V2H), Vehicle-to-Load (V2L), and Vehicle-to-Vehicle (V2V) [28]. In this way, the cars are seen as dispatchable and flexible means of power supply that can interconnect the fuel sector and the electricity sector. In 1997, Kempton et al. had already envisioned that EVs, whether fuelled by batteries, liquids or gaseous fuels generating electricity on-board, would have value to electricity utilities as power resources [29]. This opens the possibility of EVs participating in demand-side management, voltage and frequency regulations, spinning reserve, active/reactive power compensation, load balancing and harmonic filtering [30].

In the literature, V2G related research is widely correlated and usually exclusively linked to battery-run electric vehicles (BEVs)

[31,32], mainly due to the fact that FCEVs are not treated as electric vehicles and their penetration into the market has been slow in the last decades. However, this is currently changing, as most of the large car manufacturers are already commercializing FCEVs, such as the Hyundai Tucson Fuel Cell SUV [33], the Toyota Mirai [34] and the Honda Clarity [35]. In 2017, Mercedes Benz has even announced the GLC F-CELL, a plug-in FCEV that combines both a high-capacity 9 kWh battery and fuel cell technology [36]. The commercially available FCEVs have the advantage over BEVs in that they can be refuelled faster (in 3 min on average) and provide greater driving ranges of around 500 km. FCEVs are also electric vehicles and can be used in V2G as the source of new power generation, provided the correct connection interface. Several FCEV manufacturers have already developed devices to export up to 9 kW power from vehicles to electric appliances (V2L) and directly to homes (Vehicle-to-Home or V2H), and are offered as supplementary devices [37,38]. Nonetheless, there are very few studies that have considered FCEVs in V2G mode. Early works analysed theoretically the use of FCEVs as distributed power generators and evaluated their economic aspects in different electricity markets [39–43]. Recently, other works have been published on the use of FCEVs to balance building/community energy consumption, all based on theoretical assumptions about how the FCEV operates in V2G conditions [44–48]. Until now, there have been no experimental validations of such a system, which we will refer to as FCEV2G (Fuel Cell Electric Vehicle to Grid).

For the first time, we connected a FCEV to the Dutch national grid, allowing the car to deliver up to 10 kW direct current (DC) power output.[1] Our study aims to determine the potential of a hybrid microgrid system composed of FCEVs for both transportation and V2G, rooftop solar panels and all-electric housing. We focused on how the use of the FCEV2G could reduce electricity imported from the grid, with the aim of obtaining a more self-sufficient all-electric dwelling, where the energy for heating, cooling, hot water and electricity was taken into account. In addition, we examined the operational aspects of the system, in terms of the availability of the car on-site and the impact on the energy bill for the end-user.

The system was developed as a small-scale project with one house and one FCEV, since it can already be realized with available technology. In addition, a microgrid system incorporating 10 all-electric houses and 5 FCEVs was simulated for an entire year to determine annual performance. The monitoring of the real system provided data that was used in the simulated case study. Fig. 1 shows the relationship between the experimental and simulated case study and the flow of data between studies performed. These types of innovative pilot projects are pivotal in realizing the transformation of socio-technical systems such as the energy system because they actually use the innovation and thereby learn about new needs, which allow policymakers to create regulatory frameworks that fit the innovation and industrial actors to learn how to improve the innovation and reduce costs [49]. In particular, understanding how home occupants interact with their energy needs is a key consideration for all green building planning, design, operation and decision-making. Furthermore, this demonstration project allowed the analysis of real-world empirical data on load demand and PV and FCEV power supply.

The remainder of this paper is structured as follows. In Section 2, the case study of a FCEV2G-PV-HOUSE microgrid system is introduced and the energy performance of the main components is analysed. Also, the results of a two-week demonstration experiment of the hybrid system operating in real life are presented. Section 3 presents an annual simulated case study of the performance of a hybrid microgrid system with 10 houses and 5 FCEVs under different FCEV2G working modes. Finally, in Section 4, the conclusions are presented and

recommendations for further research are provided.

## 2. Case study

### 2.1. System description

The structure and components of the hybrid system under analysis in this work are represented schematically in Fig. 2. The four main components of the microgrid are the building-integrated photovoltaic (BIPV) installation, the FCEV used for mobility and power generation in V2G mode, the residential load and the electrical grid.

The operating scheme of the microgrid is as follows: while available, PV power is used to cover the load directly (direct solar). The load is considered to be the energy consumption of the house for heating, cooling, hot water and electricity, with electricity being the only energy carrier, since it is an all-electric house. In the case of PV shortage, and if the car is available on-site, the FCEV provides power to the load through the V2G connection at a fixed and constant power output that the user selects between 0 and 10 kW DC. If excess power from either the PV or the FCEV is available, electricity is fed back into the main grid through the connection in the house (export). In the case of a shortage from either distributed energy generator, electricity is drawn from the main grid (import). The main grid considered is the Dutch National grid, which has 12.5% of renewable electricity in its generation/production mix [50]. The FCEV is also used for mobility and is fuelled mainly at one of the hydrogen refuelling stations available in The Netherlands. At the time of the experiments, there were only two hydrogen stations available in The Netherlands. One is located in Helmond [51] and is a fully electric powered hydrogen station, where "green hydrogen" is produced on-site by water electrolysis and compressed to refuelling pressure. The operators of the hydrogen station in Helmond confirmed that they have a power purchase agreement with a zero $CO_2$ electricity provider. The other station, located in Rhoon offers "blue hydrogen" [52]. At this hydrogen station, the hydrogen is sourced from steam-reformed natural gas with $CO_2$ capture and connected to the industrial pipeline network of Air Liquide [53] and includes multiple hydrogen sources. The captured $CO_2$ is used in other chemical processes. This could potentially result in zero $CO_2$ emission hydrogen production. The technical possibility to refuel green hydrogen, and thus be a $CO_2$ neutral process, is available in The Netherlands today. To show the renewable potential of the concept and the related modelling study done, the hydrogen used to refuel the FCEV is considered to be $CO_2$ neutral, as the technology is available and could be applied anywhere. The components of the system were deliberately chosen based on the fact that they are all commercially available energy products and services that a home occupant or end-user can acquire and use today, given the proper connections.

The FCEV used is an ix35 Hyundai, which is an electric vehicle that uses a proton exchange membrane (PEM) fuel cell (FC) stack to convert hydrogen and oxygen into electrical power and water. In addition to the FC stack, there are auxiliary components to support the correct operation of the FC and the vehicle, such as a hydrogen and air management system, fuel cell and power electronics cooling system, and power electronics. All of these systems are grouped under the term Balance of Plant (BoP). In driving mode, the FC power is used to drive the electric traction motor. It has a 700 bar hydrogen storage tank that provides a driving range of 550 km [54].

In cooperation with Hyundai and Accenda B.V., and in the scope of the Car as Power Plant Project [55], an ix35 FCEV was provided with a power output socket, which allows for the electrical power generated by the fuel cell to be directed to a discharge unit (V2G unit) instead of the motor. A description of the setup and operational performance results can be found in [56]. When parked, the car can be connected through a cable to the V2G unit (see Fig. 3a), which allows conversion of the DC power from the vehicle to AC power and synchronization with the AC grid. To the best of the authors' knowledge, this is the very first

---

[1] This research is embedded in the Car as Power Plan Project at The Green Village in the Netherlands, which seeks to evaluate the potential of parked fuel cell electric vehicles as tri-generation systems capable of producing electricity, water and heat [55].
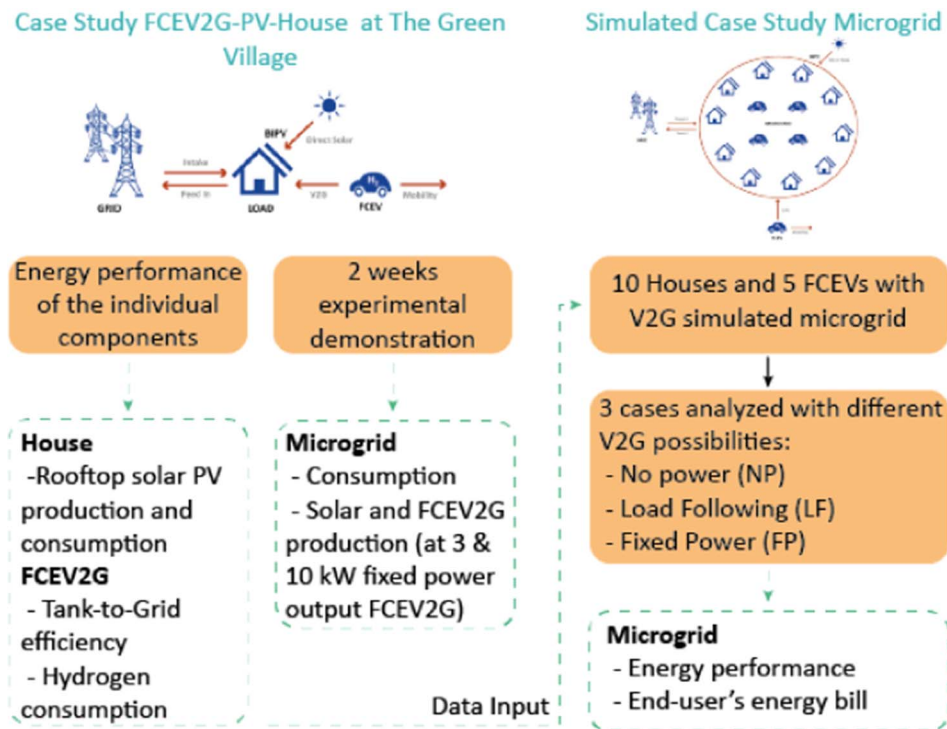
Fig. 1. Schematic diagram of the present research's structure. Stripped green line blocks represent data generation from each section and the stripped green arrow represents flow of data. (For interpretation of the references to colour in this figure legend, the reader is referred to the web version of this article.)
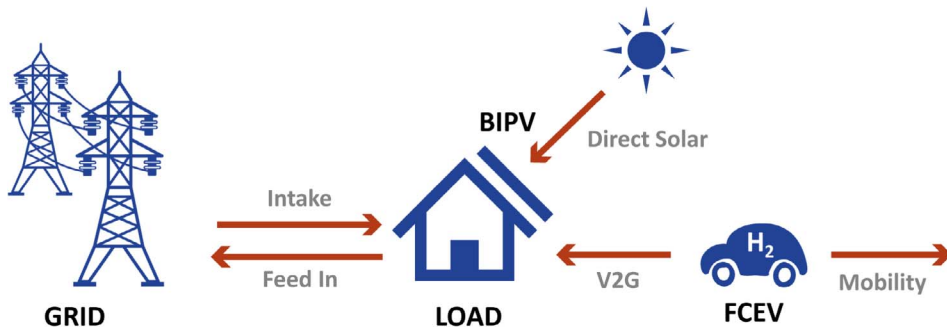


Fig. 2. Schematic drawing of the hybrid system under analysis with hydrogen FCEV, BIPV solar production, a residential load and the grid. The arrows represent the energy flows between the components.
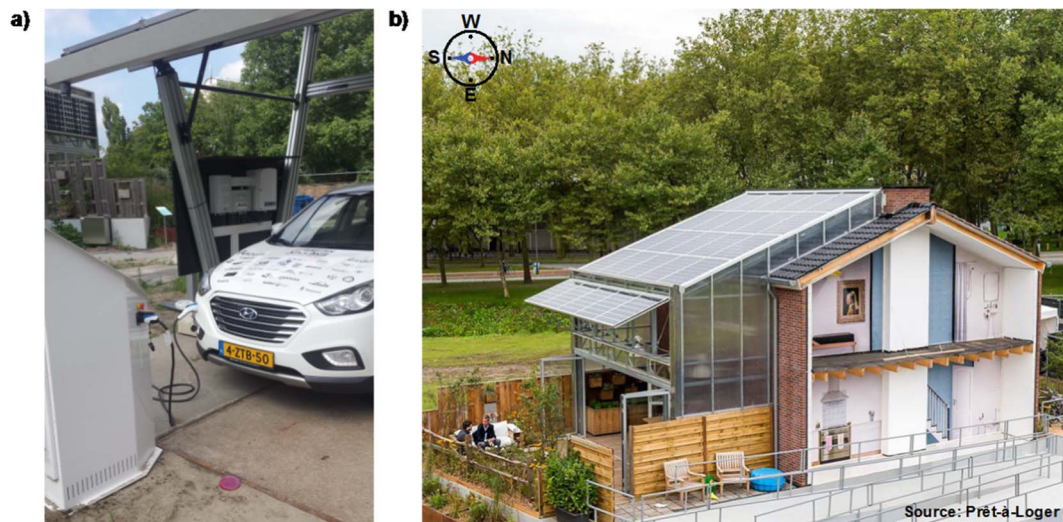


Fig. 3. (a) Photo of the ix35 Hyundai FCEV connected in V2G mode, delivering power to the grid and (b) the Prêt-à-Loger house at The Green Village. (For interpretation of the references to colour in this figure legend, the reader is referred to the web version of this article.)

time that a hydrogen FCEV has been able to deliver electricity to a national grid. Modulation of the power output can be achieved from 0 to 10 kW DC.

The residential load considered in this case study corresponds to that recorded at the Prêt-à-Loger (PaL) [57] house shown in Fig. 3b. The building is a typical Dutch terraced house that has been adapted to make it more energy efficient. The main changes consist of thermal insulation in the facade and roof, a greenhouse structure to the southeast, and phase change materials in the crawlspace [58].

The house project was designed by a team of students from Delft University of Technology (TU Delft) for the Solar Decathlon Europe 2014 competition and it is now located on the TU Delft campus at a site called The Green Village. The building is mainly used as an office and exhibition house. Less frequently, and for research purposes, it is at times temporarily inhabited by University students or staff. It has 43.6 m$^2$ of PV panels, 5.4 m$^2$ of solar thermal panels, for domestic hot water and central heating, connected to an (air) source heat pump with a nominal rated output of 4 kW and COP of 2.5–3.5, depending on the ambient/outside temperature. The building has a surface area of 116 m$^2$ (including the greenhouse surface) and it only has a bidirectional electricity grid connection, no natural gas or district heat grid connection, thus making it an all-electric house.

The BIPV system is installed on the roof and on the greenhouse window with a capacity of 4.9 kWp (4.7 kWp actual functionality because one panel was malfunctioning in 2015). It is composed of 25 modules with 1170 monocrystalline silicon solar cells in total. The modules are all connected in series to power optimizers to ensure maximum power point tracking. The total system is connected to an inverter to convert the DC output of the PV string to AC (230 V, 50 Hz, single phase). The electricity consumption and PV production of the PaL house have been constantly monitored and recorded since 2015.

## 2.2. Energy performance of the individual components

Several performance parameters of the single components, namely the PaL house with BIPV system and the FCEV2G setup, were evaluated before integrating them into the entire system. All data processing was performed offline using the commercial software MATLAB® (R2016b, 64-bit). The parameters are defined and results are presented below.

### 2.2.1. PaL house

The energy performance of the house is based on the data collected in 2015, as most of the consumption data from 2016 was lost due to a server problem. The power consumption ($\overline{P}_{cons}$) was available with a 15 min time resolution, while the PV power produced ($\overline{P}_{PV}$) was directly measured at the inverter and also available with a 15 min resolution. The annual energy consumed and produced were calculated according to Eqs. (1) and (2), respectively:

$$E_{cons,a} \ [kWh] = \int_{t_1}^{t_2} \overline{P}_{cons}(t)dt \tag{1}$$

$$E_{prod,a} \ [kWh] = \int_{t_1}^{t_2} \overline{P}_{PV}(t)dt \tag{2}$$

where $P(t)$ is the power at a given time, $dt$ is the time resolution and, depending on initial time, $t_1$, and final time, $t_2$, the energy calculation can be done on a daily, monthly or yearly basis. The 2015 production and consumption patterns of the house can be observed in Fig. 4a.

Although the house was not constantly inhabited by a family, the consumption and production patterns correspond well to those of Dutch households as reported by Reinders et al. [6]. There is a clear mismatch between production and consumption during the year. While production peaks in the summer months, when there is more radiation from the sun, consumption peaks in winter, given the higher demand for space heating and domestic hot water (DHW). The predominant component of electricity consumption in this house is the heat pump.

The total electricity consumption in 2015 for the house was 5972 kWh, while the average value in the Netherlands for the same year was 2980 kWh [59]. The value reported in this work is higher than the Dutch average electricity consumption because the latter does not take into account electricity used for heating. For a building, implementing an electric heat pump would mean that externally base electricity consumption will be considerably higher than normal because electricity is the only energy carrier that is implemented in the building [60].

With respect to the PV system, the amount of electricity generated in 2015 was 3768 kW, which accounts for a specific yield value of 802 kWh/kWp. The average specific yield in the Netherlands was reported to be 875 kWh/kWp, with variations as large as 16% [61]. Therefore, the value obtained for the PaL house can be said to be lower than the average but still within the limits. This is because the orientation of the PV system reflects the orientation of the house, which in
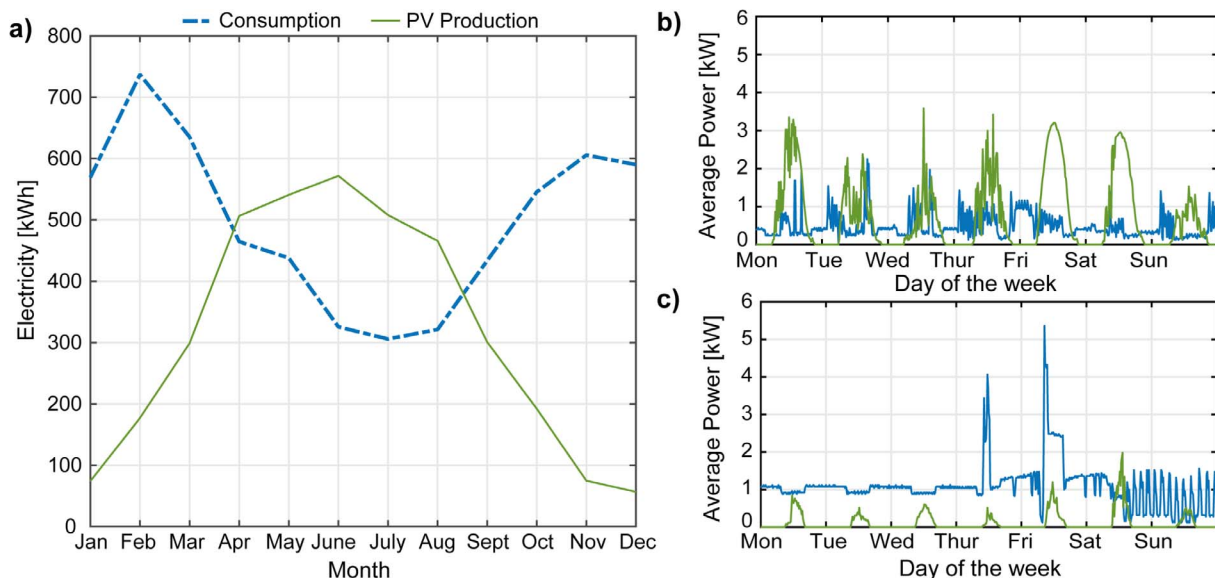


**Fig. 4.** (a) Electricity consumed (blue line) and produced (green line) by the PaL house during 2015, (b) consumption (blue line) and PV production (green line) load profiles of week 28, during summer, and (c) during week 4, in winter. (For interpretation of the references to colour in this figure legend, the reader is referred to the web version of this article.)

this case is not optimal to achieve a maximum yield (there is a 42 degree deviation from the south). In addition, the tilt of the solar system panels is also not optimal, at 21 degrees, as opposed to the optimal of 36 degrees in the Netherlands.

By looking at a random weekly profile in the summer (Fig. 4b), it can be established that during the day, the total on-site daily production is sufficient to cover the total daily load but at night the house relies entirely on import power from the grid. In the winter (Fig. 4c), solar production is much less, and is not even sufficient to cover house consumption during daylight hours. The bar chart in Fig. 5 (left y-axis) shows the origin of the electricity consumed monthly in 2015, as well as surplus solar electricity that was exported. From this plot, it can be observed that in summer less electricity was imported from the grid and relatively more solar electricity was directly used, with more solar electricity exported.

In order to evaluate the energy performance of the system in providing and using its own generated electricity, the on-site electrical energy fraction (OEFe) and the on-site energy matching (OEMe) indicators were calculated as defined by Cao et al. [46] The OEFe indicates the proportion of the demand which is met directly by on-site generation rather than being imported from the grid (grade of *autonomy*), and the OEMe indicates the proportion of on-site electrical generation which is locally consumed rather than being exported, or the grade of *self-consumption*. Their mathematical expressions are given in Eqs. (3) and (4), respectively:

$$OEFe = 1 - \frac{E_{imp,t}}{E_{cons}}, \quad 0 \leqslant OEFe \leqslant 1 \tag{3}$$

$$OEMe = 1 - \frac{E_{exp,t}}{E_{prod}}, \quad 0 \leqslant OEMe \leqslant 1 \tag{4}$$

where $E_{imp,t}$ and $E_{exp,t}$ are the imported and exported electricity to and from the grid, respectively, in the time frame $t$. The ideal behaviour of the system is achieved when both indicators equal 1, meaning that the residential load is covered entirely by on-site generation and no electricity is being exported. The monthly OEFe and OEMe values for PaL in 2015 are plotted on the right y-axis in the plot shown in Fig. 5. The OEFe values range from 0.05 and 0.44 and peak in the summer months, while the OEMe values range from 0.26 to 0.76, where higher values were obtained in the winter months. This indicates that in the summer months there was a higher direct coverage of the house load by on-site production (high OEFe), but that also more electricity was exported to the grid (low OEMe), in comparison with the winter. The same seasonal pattern was observed in the simulations performed by Cao et al. for the case with PV [46].

Net electricity consumption in this study was based on the load/generation balance as calculated in Eq. (5), which had to satisfy the inequality in Eq. (6) in order to fulfil the NZEB condition.

$$E_{net,a} \ [kWh] = E_{cons,a} - E_{prod,a} \tag{5}$$

$$E_{net,a} \ [kWh] \geqslant 0 \tag{6}$$

If Eq. (5) indicator is equal to 0, then the building is considered to be an NZEB, while if it is greater than 0 it is considered to be a positive-energy building. To compare the energy performance of the house to other residential buildings, the net annual primary energy consumption per unit of building surface area ($PE_{net,a}$) was calculated according to Eq. (7).

$$PE_{net,a} \left[ \frac{kWh}{m^2}/year \right] = \frac{PEF \times E_{cons,a} - PEF \times E_{prod,a}}{area\ building\ [m^2]} \tag{7}$$

By multiplying the electricity consumed and produced by the primary energy factor (PEF), it is possible to account for the entire energy chain, including properties of natural energy sources, conversion processes, and transmission and distribution grids. There are various methods to calculate the PEF of electricity [62]. In Eq. (7), the default

EU PEF of 2.5 is used due to the highly interconnected European electricity grid. The Default PEF of 2.5 is based on an average, European-wide conversion efficiency of 40% [63]. In this case, equal values for PEF for both consumed and produced quantities were used. This was done as it is difficult to establish a specific value for the PEF for combined solar and FCEV power generation. Partly due to the renewable component of solar energy but also the use of blue hydrogen as energy carrier, which is produced outside of the system boundaries in this work. It is assumed that the electricity produced on-site, whether self-consumed or exported, will avoid an equivalent generation of fossil based electricity somewhere in the energy infrastructure. This is due to the priority dispatch of variable renewable energy sources in the European electricity grid as established by the European renewable energy directive [64]. In 2015, the PaL house had a $PE_{net,a}$ of 47 kWh/m². The majority of the EU member states aim for 45–50 kWh/m²/y for primary energy consumption in residential buildings, while Denmark aims as low as 20 kWh/m²/y [65]. This characterizes the PaL house in 2015 as a *nearly* zero-energy building but not a *net* ZEB.

### 2.2.2. FCEV2G

To evaluate the performance of the FCEV2G connection, field test measurements with the adapted Hyundai ix35 FCEV were conducted at four different power outputs. The FCEV was connected to the V2G unit as shown in Fig. 3a, making sure that none of the energy consuming applications of the car were switched on (radio, air conditioning, heating, etc.). It is essential to point out that 'power output' refers to the DC power output of the FCEV that reaches the discharge unit. At the discharge unit there is an inverter that converts the DC power to AC power with 95% efficiency. Thus, the AC power delivered to the grid is 5% less than the FCEV's power output. Several tests were performed setting the V2G power output ($P_{V2G}$) to 1, 3, 5 and 10 kW DC constant values. Each test was repeated five times for statistical purposes. During the tests, different variables were measured, such as average fuel cell DC power produced ($\overline{P}_{FC}$), average AC power delivered to the grid ($\overline{P}_{AC}$), hydrogen mass consumed ($m_{H2}$) and duration of tests.

The system performance was analysed based on the experimental hydrogen consumption rate ($H_{2rate}$) and tank-to-grid (TTG) efficiency ($\eta_{TTG}$). The $H_{2rate}$ was obtained for each test according to Eq. (8):

$$H_{2rate} \ [kg/h] = \frac{m_{H2}}{\Delta t_{test}} \tag{8}$$

where $m_{H2}$ was obtained by measuring the difference in mass in the
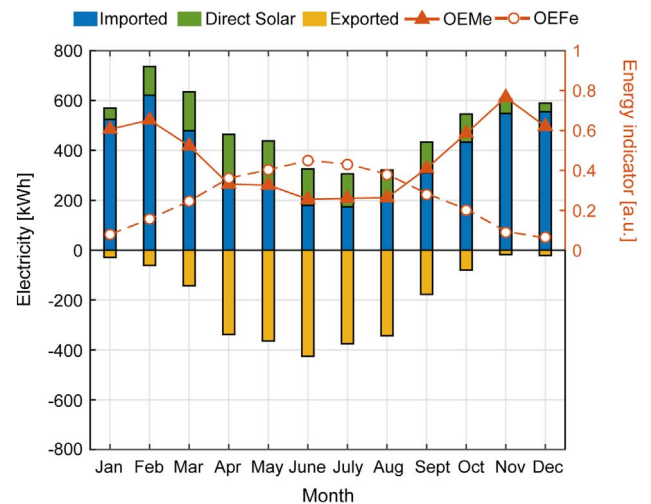


**Fig. 5.** Bar chart showing the electricity consumed monthly (positive values, stacked by origin of supply) and excess electricity exported to the grid (expressed as negative values) by PaL house in 2015. The left y-axis corresponds to the electricity values, the right y-axis corresponds to the energy performance indicator values, namely the monthly OEMe (triangle data points) and OEFe (circle data points).

hydrogen tanks before and after the test and $\Delta t_{test}$ was the duration of the test in hours. TTG efficiency expresses the conversion of $H_2$ chemical energy into AC electric energy delivered to the grid. It accounts for all the losses associated with the entire power generation and delivery system. TTG efficiency ($\eta_{TTG(H_2 \rightarrow ACgrid)}$) was calculated according to Eq. (9):

$$\eta_{TTG(H_2 \rightarrow ACgrid)} \, [\%HHV] = \frac{\overline{P}_{AC}}{\frac{m_{H_2}}{\Delta t_{test}} \cdot \frac{HHV_{H_2}}{M_{H_2}}} \times 100\% \tag{9}$$

where $m_{H_2}$ is the hydrogen mass expressed in grams consumed in the test, $\Delta t_{test}$ is the test duration in seconds, $HHV_{H_2}$ is the higher heating value of hydrogen equivalent to 285.84 kJ/mol, and $M_{H_2}$ is the molar mass of molecular hydrogen of 2.016 g/mol.

Regression analysis was adopted to evaluate the trends in the measured data for the hydrogen consumption rate and TTG efficiency. The empirical expressions resulting from the diverse regression analysis provide novel model equations of FCEV2G performance useful for future modelling and simulation work. These are used in Section 3 below in the simulated case analysis. The resulting scatter plots with their corresponding fitting lines are shown in Fig. 6. The model equations with the optimized coefficients are shown in Eq. (10) and in Eq. (11).

$$\eta_{TTG(H_2 \rightarrow ACgrid)} \, [\%HHV] = \frac{47 \times P_{V2G}}{0.7 + P_{V2G}} \tag{10}$$

TTG efficiency decreases sharply at very low power outputs (see Fig. 6a) and increases non-linearly, stabilizing at approximately 44% for higher power outputs. The lower TTG efficiencies at lower power outputs can be explained by the relatively higher BoP consumption, such as minimum coolant pump flow, anode recycling and air blower. This behaviour was also reported by Eberle et al. when they evaluated FC system efficiency in a fleet of FCEVs in driving mode [66]. In the latter case, the losses were all due to BoP components, as there was no DC to AC conversion.

It is important to determine the rate at which hydrogen is consumed in the V2G experiments, since there is a fixed amount of approximately 5 kg of hydrogen available for V2G operation in the Hyundai ix35 FCEV. Fig. 6b shows that the hydrogen consumption rate increased linearly with the power output. The resulting regression model, as shown in Eq. (11), has a high R-squared value ($R^2 = 1.0$), indicating that the variations in $H_2$ consumption are very well explained by variations in the delivered power output.

$$H_{2rate} \, [kg/h] = 0.04 + 0.05 \times P_{V2G} \tag{11}$$

The y-intercept value is non-zero, as can be seen from Eq. (11) and from Fig. 6b. At 0 kW V2G power output, no electricity is being delivered to the grid and TTG efficiency is 0% (Fig. 6a). However, when the car is in idling mode, there is a slight hydrogen consumption of 0.04 kg/h to provide electricity for the Balance of Plant. Based on the average hydrogen consumption rate obtained at the different power outputs, it can be established that 5 kg of hydrogen can deliver approximately 52 straight hours of V2G at 1 kW power output and 9 h at 10 kW power output.

Overall, the system performance below 3 kW becomes significantly less efficient than at higher power outputs, as there are too many losses associated with the BoP and DC/AC conversion in comparison to the electricity being produced at higher power outputs. Above 3 kW, the efficiency of the system practically remains unvaried. While efficiency can be gained by delivering at higher power outputs, this comes at the expense of having less operating hours available because of the higher hydrogen consumption rate. The choice is left to the users to meet their requirements, whether in terms of efficiency or the amount of hydrogen to use (this will affect the costs and also total use of the V2G connection).

### 2.3. Experimental demonstration of FCEV2G-PV-HOUSE integrated system

The following experiment was performed to better understand the matching capabilities of the FCEV2G system and how it might reduce the electricity imported into a residential building. For a period of two weeks, two people lived in the PaL house and used the Hyundai ix35 FCEV for mobility and power generation. During this period, they generated realistic load profiles by switching on/off appliances and leading a regular life in the house. As the car has a maximum storage capacity of 5.6 kg hydrogen, 3 kg per day was set as the maximum amount of $H_2$ to be used for V2G, leaving more than enough hydrogen to also meet the daily driving requirements. Refuelling was performed every day at the hydrogen refuelling station in Rhoon, the Netherlands. In the research design, and based on the previous FCEV2G experimental results (see Section 2.2.2), two different power outputs for the car were considered: during the first week, the car was connected in V2G mode at a constant 3 kW for a longer period of time, while during the second week, it was connected at 10 kW but for less time. This was fixed, meaning that the car used approximately 3 kg of hydrogen in V2G mode each day. Table 1 summarizes the operational conditions of the FCEV during the two-week experiment.

The schedule presented in Table 1 was followed as thoroughly as possible, although there were some variations, as are bound to occur in real-life situations. All of the power flows in the system were recorded and are shown in Fig. 7a. The consumption profile presents a constant base load between 1.0 and 2.0 kW. This corresponds to the appliances that were always on, such as the refrigerator and the heat pump. As the
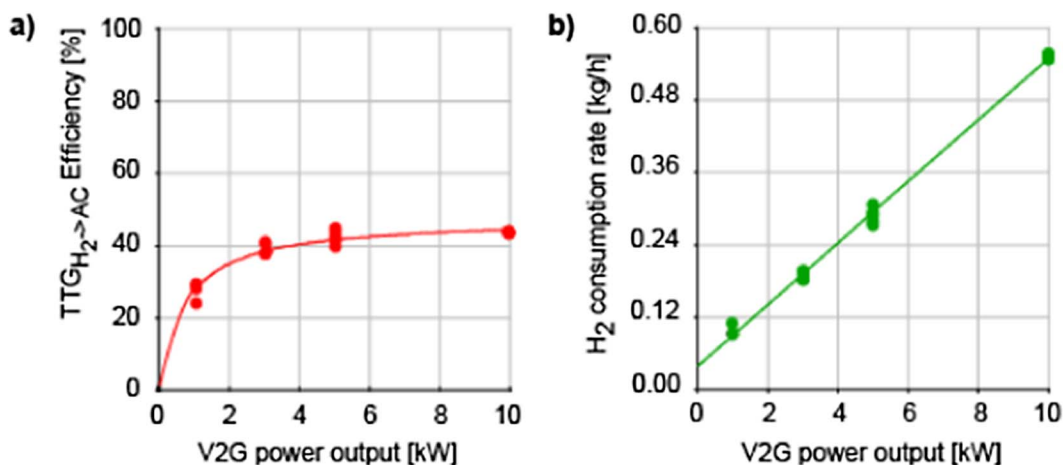


**Fig. 6.** Scatterplot of FCEV2G experimental data (points) and fitted regression analysis (line) for (a) TTG efficiency in converting hydrogen to AC electricity based on HHV and (b) hydrogen consumption rate in V2G mode at different power outputs.

**Table 1**

Operational conditions of the FCEV during the two weeks of the demonstration experiment integrating a FCEV in V2G to assist residential electricity demand.

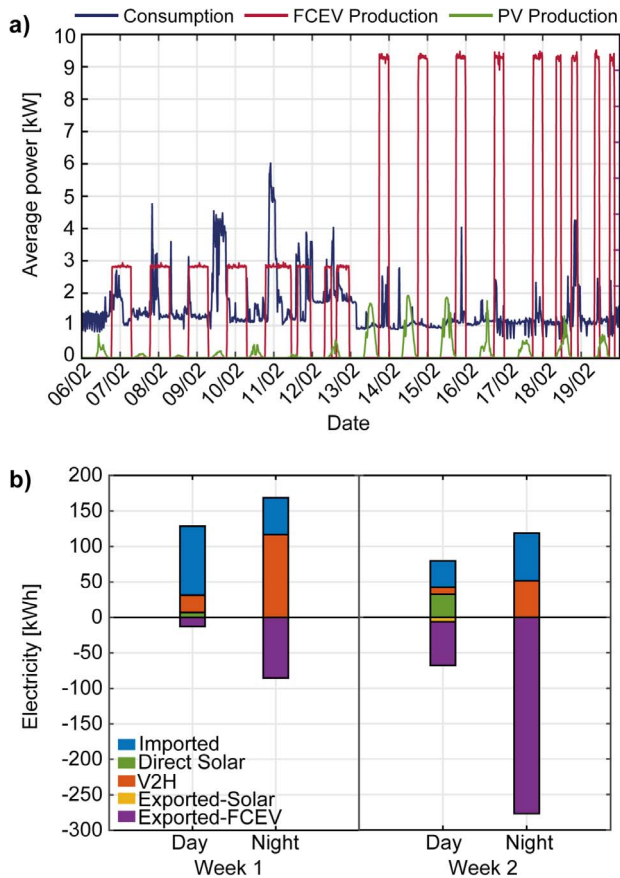|  | Week 1 | Week 2 |
|---|---|---|
| Power output | 3 kW | 10 kW |
| Schedule V2G weekday | 19–7 h (12 h in total) | 18–24 h (6h in total) |
| Schedule V2G weekend | 8–12 h and 15–23 h (12 h in total) | 8.30–11.30 h and 18–21 h (6 h in total) |



**Fig. 7.** (a) Electrical power consumption of the PaL house (blue line), solar PV production (green line) and FCEV in V2G mode electricity production (red line) for the two-week case study. (b) Bar chart showing the electricity consumed weekly (positive values, stacked by origin of supply) and excess electricity exported to the grid (negative values, stacked by origin of supply) differentiated by day and night periods. (For interpretation of the references to colour in this figure legend, the reader is referred to the web version of this article.)

experiments were performed in winter, the base load is relatively high. In addition, the first week presents higher base loads than the second week, an effect that can be explained by the heat pump having to work harder because outside average temperatures were lower for that week (see average temperatures in Table 2). This is also reflected in the total electricity consumed: under the test conditions, in the first week, 297 kWh were consumed and in the second week, 198 kWh. This can be seen in Table 2, which presents the energy performance results per week.

The first week was also cloudier, leading to very low solar PV production. From the power flows in Fig. 7a, it is interesting to note how solar PV and FCEV power production complement each other. During the day, the solar panels produced electricity, while during the night the FCEV did so. This is explicitly shown in Fig. 7b, which presents the origin of the consumed and exported electricity separately for day and night. The 'daytime' was considered to be from 8 am to 6 pm –

the period of sunlight during the experiment. The terms 'imported', 'direct solar' and 'V2H' in Fig. 7b refer to electricity imported from the grid, solar electricity produced on-site and directly used, and electricity produced by the FCEV and directly used by the house (V2H), respectively.

This figure shows that electricity consumption was higher during the night than during the day. This is due to the fact that the people living in the house were students, who were not present most of the day and their most energy intensive practices thus occurred during the night. The load was not met by the local electricity production either during the day or the night, and electricity had to be imported from the grid. During the day, there was a contribution from the solar panels but during the night it was mainly the FCEV that covered electricity consumption. The V2H contribution was higher in the first week than in the second, both for the day and night. This was because the car was connected for more hours during the day, thus satisfying the load for a longer period of time. The bar chart also shows the amount of electricity exported to the grid, which was the result of excess solar and FCEV electricity production. In the second week, more electricity was exported than consumed. This demonstrates the capability of the system to generate sufficient electricity for the house to satisfy the ZEB target and also to produce sufficient electricity to potentially share with neighbouring houses.

For this all-electric house in winter, in the first week, during which the FCEV2G connection was working at 3 kW, approximately 83% of the electricity consumption was produced on-site by both PV and FCEV. Thus, the NZEB target was not achieved. However, when working at 10 kW (during the second week), electricity demand was fully covered, with production sometimes more than twice that consumed, converting the house into a positive-energy building. In comparison with the energy performance of the PaL house with only PV, reported for February 2015 (Fig. 5, Section 2.2.1), the autonomy (indicated by OEFe) was greatly increased with the use of the FCEV2G setup, from approximately 15% to 50% and 47% autonomy for the first and second weeks of the experiment, respectively. The self-consumption of locally produced electricity (indicated by OEMe) was the same in the first week as the average monthly value from February 2015, but it dropped dramatically in the second week due to the amount of excess electricity produced, which had to be exported.

This experimental demonstration was useful in showing the high potential of the FCEV to provide V2G services to the residential sector and help achieve the NZEB target. Although the experiment was only performed for a short period of time, and only in winter, it provided useful data that proved the technical capability of the system. Seasonal variations in the behaviour of the system are expected to occur due to increased solar production in the summer months. In addition, the FCEV2G setup, as it is now, only allows for the possibility of fixed power settings, while it would also be interesting to evaluate variable power outputs. In the following section, we discuss a microgrid simulated over a one year period based on the previous experimental results and taking into account different operational modes for the V2G connection.

**Table 2**

Energy performance results of the two-week experiment.

|  | Electricity consumed [kWh] | Solar electricity produced [kWh] | FCEV electricity produced in V2G [kWh] | OEFe | OEMe | Average temperature High/Low [°C] |
|---|---|---|---|---|---|---|
| Week 1 [3 kW] | 297 | 7 | 239 | 0.50 | 0.60 | 2/−1 |
| Week 2 [10 k-W] | 198 | 39 | 400 | 0.47 | 0.21 | 10/2 |

## 3. Annual simulated case study for a microgrid

### 3.1. Model description and inputs

To determine the potential of V2G services provided by FCEVs in aiding all-electric residential prosumer type houses in the Netherlands to become NZEB, a microgrid model was simulated based on 10 houses and 5 FCEVs with V2G capability (considering that 1 in every 2 households has a private FCEV with V2G capability). The electricity consumption of the microgrid considered all the energy intensive practices in the houses such as heating, cooling, hot water, cooking, lighting and the use of electronic devices. The operating scheme of the microgrid is schematized in Fig. 8. The overall consumption and production profile of 10 houses and only one V2G point was taken into account.

The simulation was performed on a 15 min basis for 2015. The data previously collected for the PaL house and the Hyundai ix35 FCEV was used in the model and two different operating modes for the FCEVs were considered. All 10 houses had the same profiles as that reported for the PaL house in Section 2.2.1. In this manner, we analysed the worst case scenario, in which all consumption peaks occurred at the same time. The two operating modes for the FCEV2G setup were labelled *load following* (LF) and *fixed power* (FP). LF referred to variable power output when it was connected to the V2G discharge unit.

The power provided was exactly what the microgrid load demanded in the time step of the simulation (with a maximum output of 10 kW). The FP mode delivered a constant value of 10 kW whenever the car was connected in V2G mode. In both cases, the term V2H was used to refer to the electricity produced by the FCEV and directly used to cover the load in the microgrid; any excess electricity produced was exported to the grid (excess from this source only occurred in FP mode). The energy performance was analysed for three different cases: the two different modes of FCEV2G operation just described and a baseline case for

comparison, where there was no FCEV but where an internal combustion engine vehicle (ICEV) was used.

In summary:

- Case NP (No Power): represents 10 PaL houses with BIPV system and 5 ICEVs for transportation. There is no V2G operation.
- Case LF (Load Following): represents 10 PaL houses with BIPV system and 5 FCEVs for transportation and power generation in V2G mode with load following operation.
- Case FP (Fixed Power): represents 10 PaL houses with BIPV system and 5 FCEVs for transportation and power generation in V2G mode with fixed power operation (10 kW).

Car-sharing for transportation was not considered in any of the cases, meaning that the person who owned the car was the person that used it for mobility. However, car-sharing for V2G operation was considered since only one FCEV at a time was to be connected in V2G mode to the microgrid. When the hydrogen on board that car reached a certain limit, the next available car started delivering V2G services. In this way, the hydrogen in the tank was not a constraint for continuous V2G operation, as long as the cars were available on-site. The energy performance of the simulated cases was evaluated by means of the energy contributions, monthly OEMe and OEFe energy indicators and the energy bill with the data for 2015.

### 3.1.1. FCEV assumptions

The performance of the FCEV2G in both modes was evaluated using Eqs. (10) and (11), obtained from the regression analysis previously described in Section 2.2.2. The availability of all cars in the model was assumed to be the same. The cars were considered to be parked at home for 16 h on weekdays and 18 h on Saturdays and Sundays, as shown in Fig. 9. This is the European average 'inactive parking' time, which is considered to be the duration of time a car has been parked before the
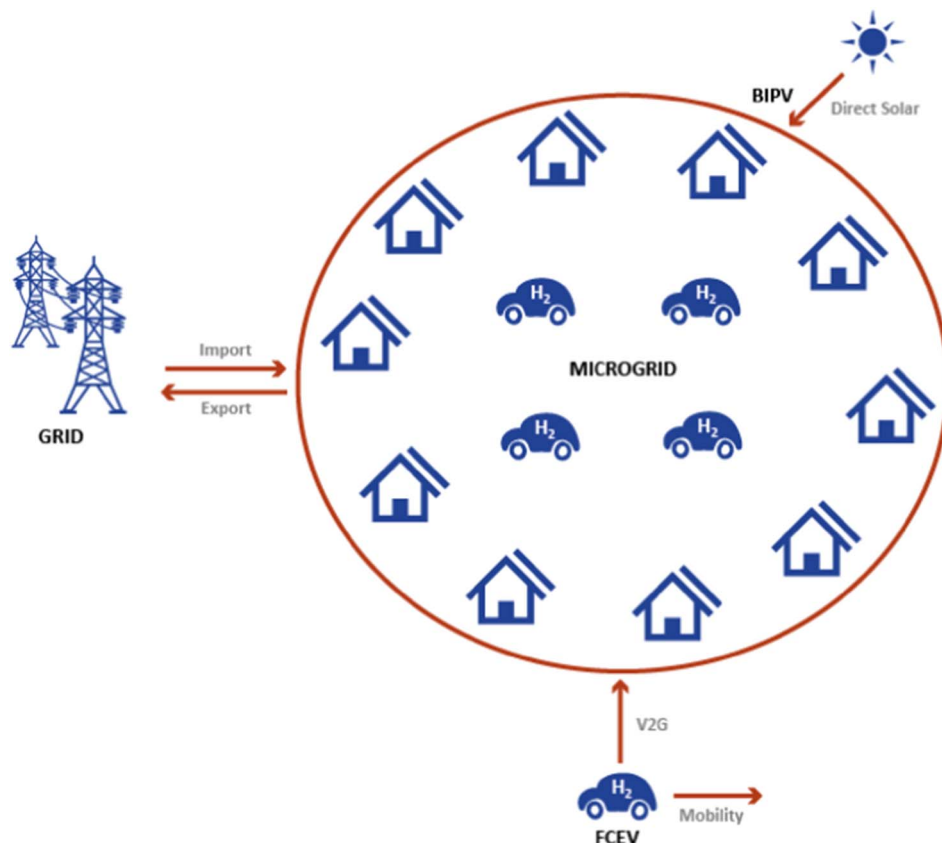


**Fig. 8.** Schematic drawing of the microgrid under analysis with 10 houses, 5 hydrogen FCEVs and BIPV solar production.
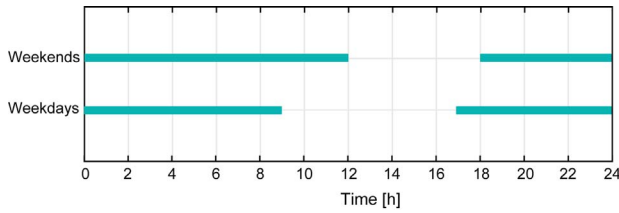
Fig. 9. Scheduled availability of the five cars in the microgrid used in the simulation.

first trip of the day or after the last trip of the day [12]. This accounts for the cars being inactively parked 88% of the time over an entire year. A sensitivity analysis was also performed to analyse the impact of the availability of the cars on the results.

Both LF and FP modes operated when the car was available and the amount of hydrogen in the tank was between 0.6 and 5.6 kg, leaving sufficient hydrogen to drive 32 km per day on average (which corresponds to the annual average distance driven by Dutch privately owned passenger vehicles in 2015 of 11,666 km [67]). When the FCEV2G was in operation, hydrogen consumption was determined by Eq. (11). When the car was absent, a homogeneously distributed driving profile was considered. The hydrogen consumed while in driving mode was calculated for every 15 min that the car was not present at home using Eq. (12):

$$H_{2driving} \ [\text{kg}] = km_{t.step} * H_{2rate.driving} \tag{12}$$

where $km_{t.step}$ corresponds to 0.6659 km driven in the 15 min time step (equivalent to 32 km in 12 h) and $H_{2rate.driving}$ is equal to 0.0095 kg/km [68].

### 3.1.2. Energy bill calculation

In this study, the energy bill was considered as the monetary cost of the amount of electricity and fuel used over the entire year. A net metering system was assumed for electricity production and consumption as established in the Netherlands. In this system, unused electricity produced on-site is fed back into the power grid and this amount of power is deducted from the electricity bill of the supplying household. In the Netherlands, there is a limit to net metering, equal to the amount of imported electricity from the grid. The energy delivered to the grid above this limit has a different tariff rate. In the calculation performed in this study, there were no considerations of investment and maintenance costs, as a cost benefit analysis of the system was not part of the scope of the study. Here, we were merely concerned with estimating how the end-user's annual energy bill might be affected, assuming that FCEVs will cost the same as ICEVs in the near future [69]. Eq. (13) was employed to perform the energy bill calculations:

$$\begin{aligned} Energy \ bill \ [\text{€}] = &(E_{imp} - E_{exp,NM}) \times P_{kWh,NM} + E_{exp,Extra} \times P_{kWh,Extra} \\ &+ km_{driven} \times \overline{Fuel}_{cons} \times \overline{P}_{fuel} + H_{2V2G} \times P_{H_2} \end{aligned} \tag{13}$$

where $E_{imp}$ is the imported electricity, $E_{exp,NM}$ is the exported electricity that applies to the net metering limit, $P_{kWh,NM}$ corresponds to the average consumer price per kWh in the Netherlands, $E_{exp,Extra}$ is the exported electricity above the net metering limit, $P_{kWh,Extra}$ is the price offered by the energy company to the end-user for the electricity

delivered above the net metering limit, $\overline{km}_{driven}$ is the average kilometres driven in 2015 for Dutch privately owned passenger vehicles, $\overline{Fuel}_{cons}$ is the average fuel consumption, $\overline{P}_{fuel}$ is the annual average price of the corresponding fuel at the pump, $H_{2V2G}$ corresponds to the average amount of hydrogen used in one year in V2G mode per car in the microgrid and $P_{H_2}$ is the average annual hydrogen price at the pump. The values used in this equation for the different cases analysed are reported in Table 3.

The energy bill was calculated for all three cases, considering a single all-electric household within the microgrid with either an ICEV or a FCEV. In the LF and FP cases, using the FCEV for driving and power generation, the cost of the hydrogen used for V2G in the microgrid was shared evenly among the 10 households. The last term in Eq. (13), a measure of hydrogen costs of V2G operations, is null in the NP case, where only ICEVs were considered without power generation. The $\overline{Fuel}_{cons}$ used for the FCEV was that reported for the Hyundai ix35 FCEV model. For the NP case, the 2016 Hyundai Tucson model was taken as the reference, which is the same car as the ix35 but with a petrol engine rather than an FC and electric powertrain. Since the hydrogen price was identified as one of the major variables affecting the energy bill, a sensitivity analysis was performed for this variable as well. This allowed the hydrogen breakeven price to be calculated; that is, where the FCEV cases would cost the same as the ICEV case.

### 3.2. Results and discussion

Fig. 10a presents the monthly electricity consumption of the microgrid, as well as the simulated on-site total electricity production in the three cases analysed. In all cases, a seasonal variation can be observed, where more electricity was produced in the summer months than in the winter months, due mainly to solar production. This shows the limitation of solar power alone to cover the power needs of the microgrid throughout the entire year. The yearly values obtained for the microgrid are reported in Table 4. For the entire year, both LF and FP cases produced sufficient electricity to cover the microgrid load, converting the houses in the microgrid to positive-energy buildings with a $PE_{net,a}$ per household of $-23$ kWh/m$^2$ and $-64$ kWh/m$^2$ for LF and FP cases, respectively. This proves the capability of the FCEV2G system to help achieve the zero-energy target for residential buildings, which could not be achieved in the NP case.

As can be seen from Fig. 10b, some of the electricity produced in the FP case had to be exported to the grid. Fig. 10b also shows the sources from which the load was covered each month. The NP case had the highest contributions of electricity imported from the grid, while these contributions were much lower in the LF and FP cases because of the FCEV2G power supply. On average, for the entire year, both LF and FP reduced the import of electricity by approximately 71% compared to the NP case. The energy performance of the three cases analysed is well explained by the variation of the OEFe and OEMe indicators over 2015, as shown in Fig. 10c and d, respectively. The OEFe values presented the same trend in all three cases, where higher values were obtained in summer than in winter, due to the higher direct solar coverage in the summer. Although they present the same trend, there is a significant increase in the absolute values for the LF and FP cases (which overlap) with respect to the NP case. This indicates a higher degree of autonomy

**Table 3**
Input data used in the energy bill calculation for the three different cases. Values correspond to data for 2015 in the Netherlands.

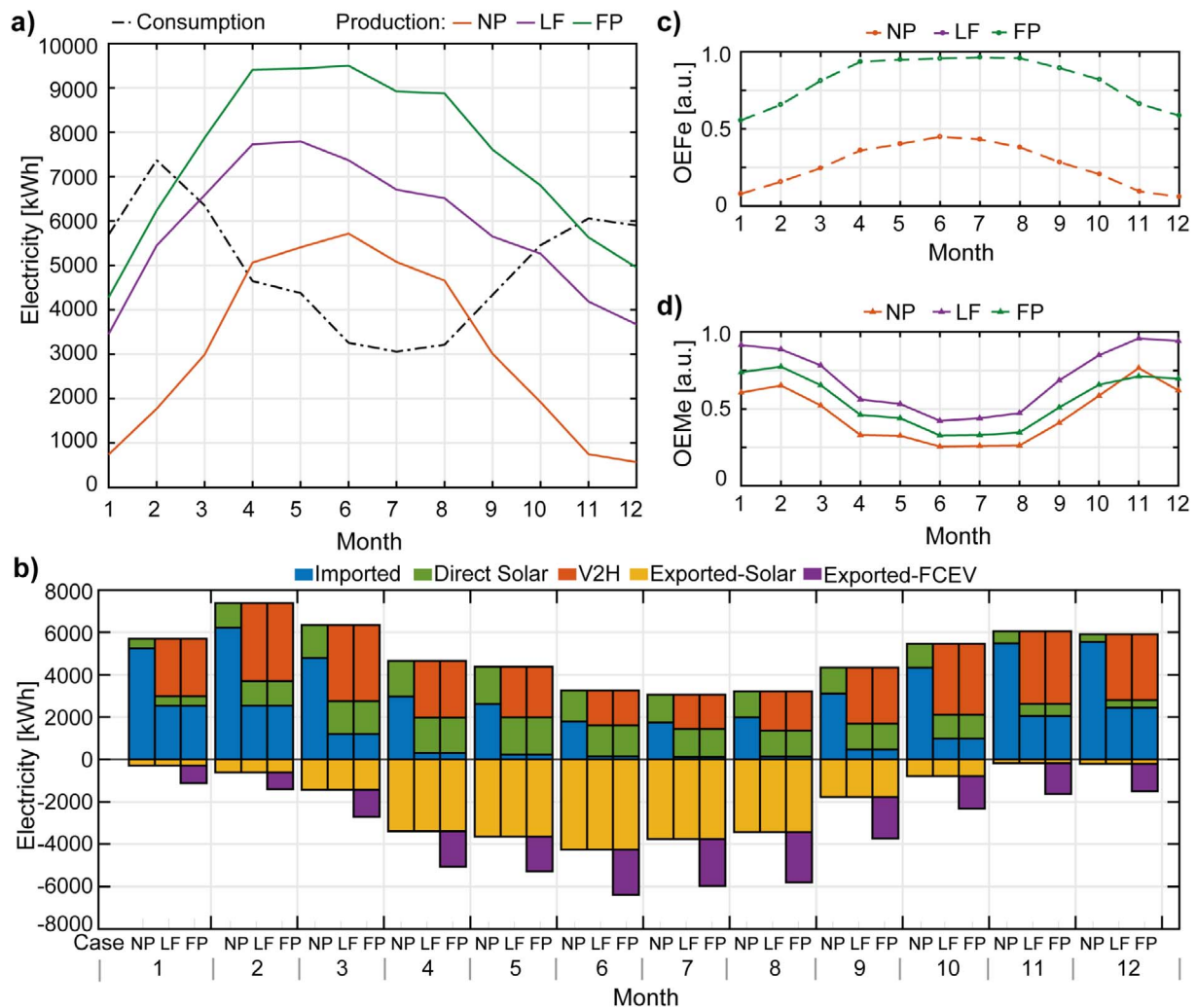| Cases | No Power (NP) | Load Following (LF) | Fixed Power (FP) |
|---|---|---|---|
| Electricity price net metering, $P_{kWh,NM}$ | | 0.183 €/kWh [70] | |
| Electricity price above net metering condition, $P_{kWh,Extra}$ | | 0.11 €/kWh [71] | |
| Annual average distance driven, $\overline{km}_{driven}$ | | 11,666 km [67] | |
| Average fuel consumption, $\overline{Fuel}_{cons}$ | 0.105 L$_{gasoline}$/km [72] | 0.0095 kg$_{H2}$/km | |
| Annual average fuel price at the pump, $\overline{P}_{fuel}$ | 1.56 €/L [73] | 12 €/kg | |

**Fig. 10.** Results of the three different cases analysed for 2015. (a) Electricity consumption (dotted line) by the microgrid and production of the simulated cases (full line); (b) Bar chart showing the electricity consumed monthly (positive values, stacked by origin of supply) and excess electricity exported to the grid (negative values, stacked by origin of supply); monthly (c) OEFe and (d) OEMe values.

**Table 4**
Entire year results of the simulated microgrid for the three cases analysed.

| Cases | No Power (NP) | Load Following (LF) | Fixed Power (FP) |
|---|---|---|---|
| Electricity consumption/kWh | | 59,719 | |
| PV production/kWh | | 37,678 | |
| FCEV production/kWh | 0 | 32,690 | 51,840 |
| Total on-site electricity production/kWh | 37,678 | 70,368 | 89,518 |
| Total electricity exported/kWh | 23,786 | 23,786 | 42,936 |
| Total electricity imported/kWh | 45,828 | 13,137 | 13,137 |
| Net annual primary energy consumption, $PE_{net,a}$/kWh/m² | 47 | − 23 | − 64 |

of the energy system with the use of the FCEV2G setup, almost reaching the value of 1 in the summer months. OEMe values were higher in the winter months for all cases and the LF case presented the best performance in terms of self-consumption, while the NP case presented the lowest OEMe values because most of the electricity produced on-site was exported.

With respect to grid interaction, it is interesting to observe the imported and exported electricity power duration curves, shown in Fig. 11. These curves are equivalent to the Load Duration Curve used in

power system analysis, which is an arrangement of all the load values over a year in descending order.

From Fig. 11a it can be seen that the use of FCEV in V2G, either in LF or FP mode, reduced the imported power values between 0 and 15 kW but did not affect the peak values between 15 and 55 kW. These peak values occurred during less than 5% of the year. In these cases, the use of batteries, either in FCEVs or BEVs and/or stationary batteries, could be used to supply the higher power demand of the microgrid. For example, by virtue of different V2G power management algorithms, the 24 kW battery present in the Hyundai ix35 could reduce these higher peaks.

While the use of FCEV2G in LF mode did not affect the power exported to the grid (Fig. 11b), the FP mode produced an increase in the exported power values between 0 and 10 kW. Although these duration curves provide useful information on the grid interaction over the year, they do not offer any insight into the daily or monthly behaviour of the microgrid. Figs. S1 and S2 (in the supplementary material) provide box plots of the imported and exported (both hourly and monthly) average power, respectively. Based on the hourly box plots (Fig. S1), it can be established that imported power diminishes during the hours of the day that the car is connected to the microgrid, in comparison with the absence of FCEVs. In the FP case, exported power also increases when the cars are connected, although the exported amount is roughly half of what was previously imported in the case without FCEVs.
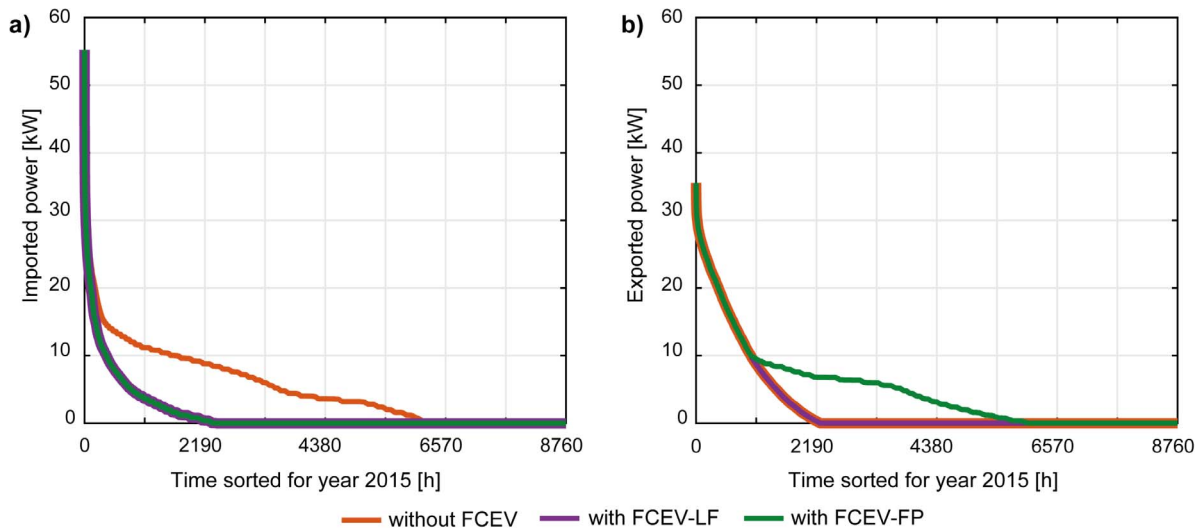
Fig. 11. (a) Imported and (b) exported power duration curves for the three cases analysed for 2015.

Based on the monthly box plots (Fig. S2), it can be concluded that the imported power was reduced all year round, but even more drastically in the winter months. This proves the capability of FCEVs to provide back-up power, especially in winter when the solar source is less capable. The exported power is incremented only for the FP case, and this is greater in summer than in winter. This is in agreement with the information provided by the monthly OEMe values, which established that self-consumption is higher in the winter months. One possible way to reduce exported power in summer would be to produce hydrogen on-site in this period and then use it in winter to fuel the FCEVs.

Combining the information provided by both energy indicators, the duration curves and the box plots, it can be concluded that the microgrid with solar PV power production and load following FCEV2G operation mode presented the best performance in terms of autonomy and self-consumption of the electricity produced on-site over the entire year. The LF mode is more interesting from the grid interaction point of view, since it responds better to demand and does not overload the grid with excess electricity.

The results on the performance of the FCEV in the LF and FP cases can be found in Table 5.

The higher TTG efficiency obtained for the FP case in comparison with the LF case can be explained by the lower power outputs that the FCEV2G setup delivered in the LF mode compared to the FP mode. The FP mode operated constantly at 10 kW and the LF mode operated at different power outputs, as can be seen from the histogram presented in Fig. 12.

The histogram shows the frequency of power produced by the FCEV2G in the load following mode for the entire year. In this mode, the V2G power output values presented a bimodal distribution, with peaks at approximately 4 and 10 kW. The two distinct values are the result of seasonal variation, with higher power outputs required to meet the load in winter and lower power outputs required in summer. Since more electricity was produced in the FP case, more hydrogen was used in the V2G mode, as can be seen from Table 5. This led to more hydrogen refuelling events over the entire year for the simulated FP case compared to the LF case. In both cases, approximately 65 refuelling events over the year were needed for driving. This means that 20 and 58 additional refuelling events were needed for the LF and FP cases, respectively, to cover V2G hydrogen demand.

In brief, the load following mode in the FCEV2G setup was less energy efficient than the constant power production configuration, but it consumed less hydrogen and required less effort from the end-user in terms of refuelling events. This conclusion is valid for the system under

study, which considered a 100 kW FC size and a part-load operation of 10% in the V2G fixed power mode. TTG efficiency could be improved if a smaller FC was used, thus incrementing the part-load operation. Recently, an FC range-extended EV has been reported that combines battery technology with a smaller FC system of 25 kW, offering great performance and autonomy [74]. This type of system should be targeted for V2G operation, as it could offer the service in a more efficient way.

Since the availability of the cars and the hydrogen price were acknowledged as the two main variables affecting the outcome of the simulation, a sensitivity analysis was performed on each, with the results shown in Fig. 13. Fig. 13a presents the energy imported and exported annually as a function of the availability of the car. A 0% change presents the base case analysed in the simulation, where the cars were available for V2G operation for 88% of the year; +12% represents 100% availability, assuming that at all times one of the 10 cars would be available; −10% change represents 72% availability (15 h on weekend days and 13 h on weekdays). The availability of the cars in either LF or FP mode had the same impact on imported energy. Full availability of the cars in the microgrid can reduce the imported energy required from the grid by half compared to the base case. However, with the limitation set at one car providing V2G at 10 kW, 0% import cannot be attained. Thus, more V2G points in the microgrid would have to be incorporated to satisfy the high peaks in demand and thereby attain 0% import. While exported energy is not affected by the availability of the cars in LF mode, it is affected in the FP mode. In the latter, with a greater availability of cars, more energy is exported to the grid.

The other variable analysed was the hydrogen price. The energy bill variation due to the hydrogen price for the three cases analysed can be seen in Fig. 13b. For the reference case (NP), we can see that the energy bill is not affected by the hydrogen price, as there is no utilization of an FCEV (and thus no reliance on hydrogen). In contrast, both LF and FP cases are greatly affected by the hydrogen price at the pump. The x-values of the crossover points of the NP case with the LF and FP cases

**Table 5**

FCEV results related to the two different FCEV2G operation modes: the Load Following (LF) and Fixed Power (FP) cases analysed.

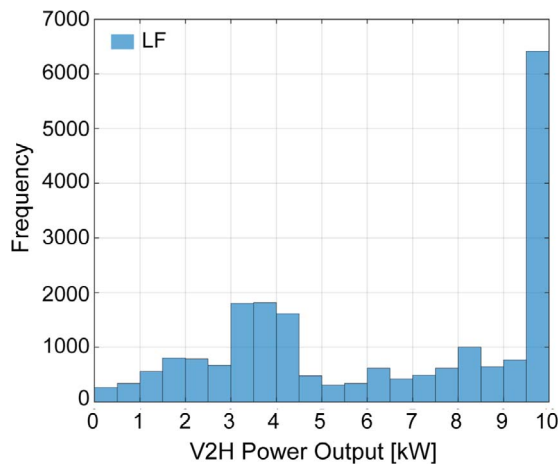|  | LF Case | FP Case |
|---|---|---|
| Annual average Tank-to-Grid efficiency (HHV) [%] | 40.7 | 44.2 |
| Average $H_2$ used for V2G per car [kg] | 368.4 | 559.9 |
| $H_2$ used for driving per car [kg] | 110.8 | 110.8 |
| Average refuelling events at $H_2$ station [number/year] | 85 | 123 |

Fig. 12. Histogram showing the frequency of power produced by the FCEV2G setup in load following (LF) mode.

are the respective breakeven prices for hydrogen for each case. This is the hydrogen price at which the system using FCEVs would cost the same as the one using ICEVs. The breakeven hydrogen price at the pump for LF mode was 8.24 €/kg, while it was 6.76 €/kg for the FP mode.

Based on these results, two different scenarios with two different hydrogen prices were analysed, assuming gasoline prices remained the same. The first scenario considered current hydrogen prices at the pump in the Netherlands of 12 €/kg and the second at 3 €/kg. The latter value is consistent with the target of the US Department of Energy (DOE) of 2–4 \$/kg for hydrogen at the pump by 2020 [75].

Fig. 13c shows the results for the two scenarios considered. The total bill is split into what corresponds to the energy bill of the car (hydrogen for driving) and what is due to the house (considering export, import and FCEV2G use). Since an FCEV is more efficient than a gasoline car for driving, the energy bill for the car component is lower in all scenarios analysed. At the current hydrogen price at the pump in the Netherlands, both cases considering FCEV2G operation are more expensive than the NP case. However, if the hydrogen price was 3 €/kg, the energy bill would have been much less for all cases of FCEV analysed. The cheapest would be the load following operation mode of the FCEV2G setup, which resulted in savings of €1546 over the year, in comparison with the NP case. Furthermore, it is not known at this point how the V2G operation would affect fuel cell degradation in real operating conditions. Combined driving and V2G test measurements over extended periods of time are needed to observe the potential degradation. Thus, at lower hydrogen prices than the actual prices, the system employing FCEV2G in supporting residential loads could be both economically attractive for the end-user and an environmentally friendly solution to decouple the energy system from conventional
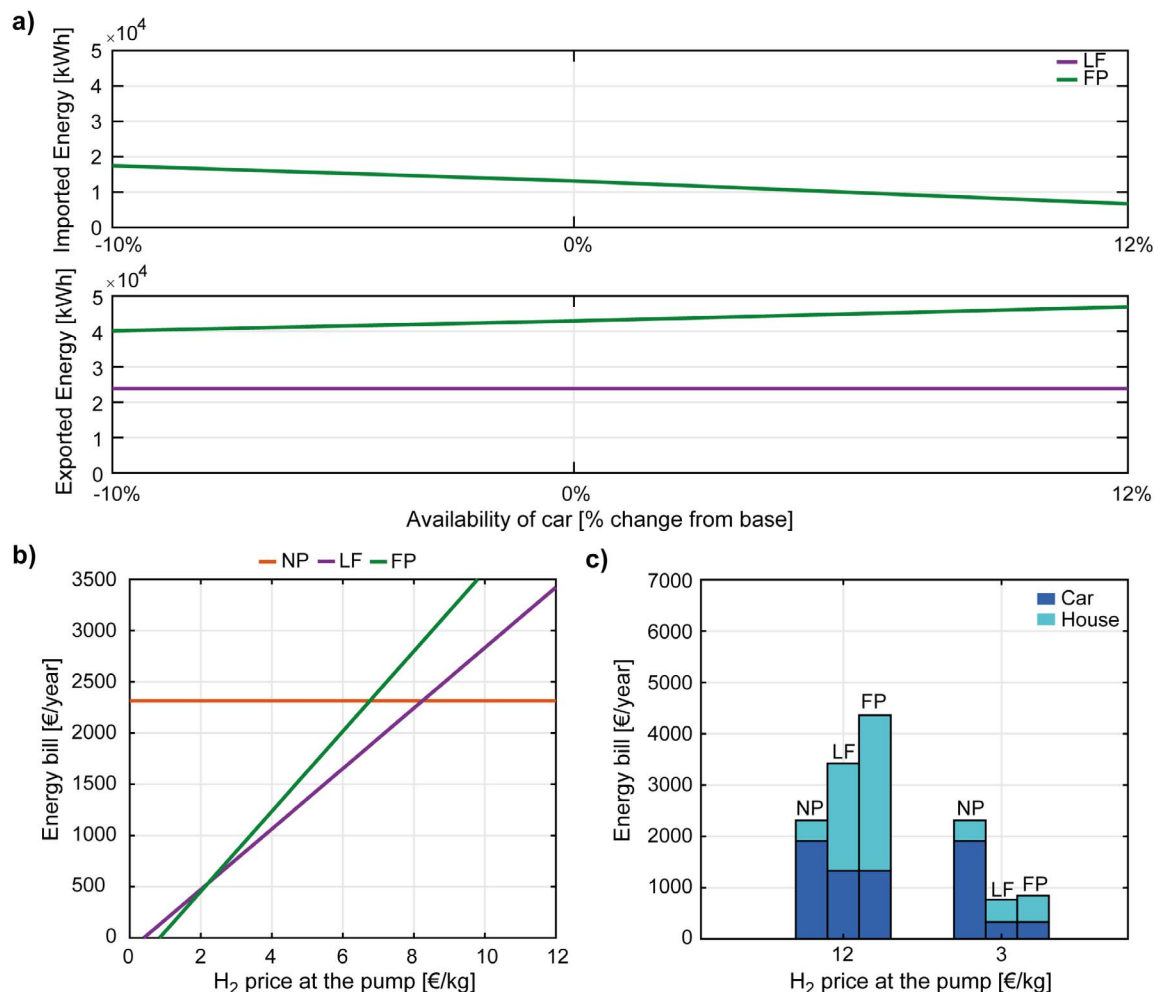


Fig. 13. (a) Variation of the energy imported and exported annually in the microgrid versus the availability of the cars on-site for the Load Following (LF) and Fixed Power (FP) FCEV2G cases. (b) Plot of the annual energy bill versus hydrogen price at the pump for the three cases analysed. (b) Bar chart of an end-user's annual energy bill for the three cases analysed, taking into account two hydrogen price scenarios. The bars are stacked to indicate which part of the bill corresponds to the car (blue) and which to the house (light blue). (For interpretation of the references to colour in this figure legend, the reader is referred to the web version of this article.)

fossil-fuel derived electricity.

## 4. Conclusions

This research has shown that parked FCEVs can provide balancing power electricity to all-electric residential buildings with BIPV and achieve the net-zero energy target. This research showed that car availability, according to European parking patterns, complements those periods of insufficient solar power, primarily at night and during winter. In this respect, a case study was conducted at the test location of The Green Village in the Netherlands and the detailed empirical data collected on the consumption of an all-electric household, PV production of a 4.7 kW system and V2G power production of a Hyundai ix35 FCEV. The performance of this microgrid was evaluated for a period of two weeks during winter, with the FCEV delivering 3 and 10 kW in V2G mode, in the first and second weeks of the experiment, respectively.

The results showed that the autonomy of the microgrid was greatly increased with the use of the FCEV2G, achieving approximately 50% autonomy in both cases. In addition, efficiency maps were made by doing tests in the range of 1–10 kW. The FCEV2G setup was found to produce electricity from hydrogen more efficiently in the range of 3–10 kW. The hydrogen consumption rate was found to increase linearly with the power output. As the electricity produced by the Hyundai FCEV with a 100 kW fuel cell, operating in the range 3–10 kW power output, is much more than needed by one dwelling, it can be used to power several houses connected in smart grids. Alternatively, FCEVs with smaller fuel cells and V2G would better match a single Dutch family house (light-weight vehicles, such as scooters or range-extended vehicles). Although it was not investigated in this study, it is thought that smart grids [76], autonomous driving [77] and self-parking cars [78] will in general facilitate the integration of electric vehicles, supplementing renewable energy supply.

Based on these experiments, a model simulating a microgrid of 10 houses and 5 FCEVs was developed and its annual performance evaluated. Two different modes of operation for the FCEV2G setup were identified: load following and constant power output. The simulation results showed that FCEV2G operation in both modes could lead to improvements in the on-site matching capability of the electricity demand of the dwellings, when compared to the system without FCEV2G operation. Savings of up to €1546 over one year on the end-user's energy bill could be achieved by using the load following power mode and sharing V2G within the neighbourhood, if the price of hydrogen at the pump dropped to 3 €/kg. At the moment, technologies coupled to the hydrogen economy, such as electrolysers, fuel cells and FCEVs are still quite expensive and from the authors' experience, there is still little awareness of these technologies and potential among general public. This poses as a challenge for users to adopt these technologies in their own homes. With the mass production of FCEVs, costs could go down and general acceptance on hydrogen could increase once the benefits of using this technology is widely seen.

The simulations considered a worst-case scenario by making the profiles of the houses all the same and the availability of the cars also the same. However, real-life variations can be expected, based on different occupation rates of the houses and different living styles of the occupants. Despite several model limitations, the results show the benefits of using FCEVs in V2G mode in a microgrid and demonstrate how the transport and residential sectors can be combined to achieve a more sustainable energy system. The complementarity of solar power and hydrogen power *via* V2G during day/night and winter/summer suggests a great potential for these two power sources to be combined in smart grids. Implications of different solar and wind resource patterns in different parts of the world and the complementarity between RES generation and FCEV2G could be subject for future research. Further possibilities for synergies between hydrogen and electricity networks should be explored, such as local hydrogen production and storage using surplus renewable solar energy production in the smart grid, and peer-to-peer hydrogen trading with local hydrogen refuelling stations. In future work we will evaluate smaller fuel cell electric vehicles, such as hydrogen scooters and light-weight vehicles to supplement houses in microgrids 'behind the meter'. This will become an interesting option for end-users to reduce their electricity bills, especially once the electricity grid becomes more renewable and the sustainability goal is met.

## Appendix A. Supplementary data

Supplementary data associated with this article can be found, in the online version, at http://dx.doi.org/10.1016/j.apenergy.2018.02.038.

## References

[1] IEA. Next generation wind and solar power - from cost to value 2016:40. http://doi.org/10.1787/9789264258969-en.

[2] Zhang X, Chan SH, Ho HK, Tan SC, Li M, Li G, et al. Towards a smart energy network: the roles of fuel/electrolysis cells and technological perspectives. Int J Hydrogen Energy 2015;40:6866–919. http://dx.doi.org/10.1016/j.ijhydene.2015.03.133.

[3] Mathiesen BV, Lund H, Connolly D, Wenzel H, Ostergaard PA, Möller B, et al. Smart energy systems for coherent 100% renewable energy and transport solutions. Appl Energy 2015;145:139–54. http://dx.doi.org/10.1016/j.apenergy.2015.01.075.

[4] Marique AF, Reiter S. A simplified framework to assess the feasibility of zero-energy at the neighbourhood/community scale. Energy Build 2014;82:114–22. http://dx.doi.org/10.1016/j.enbuild.2014.07.006.

[5] International Energy Agency. Energy technology perspectives 2016. Towards Sustainable Urban Energy Systems; 2016.

[6] Obinna U, Joore P, Wauben L, Reinders A. Comparison of two residential Smart Grid pilots in the Netherlands and in the USA, focusing on energy performance and user experiences. Appl Energy 2017;191:264–75. http://dx.doi.org/10.1016/j.apenergy.2017.01.086.

[7] Kolokotsa D. The role of smart grids in the building sector. Energy Build 2016;116:703–8. http://dx.doi.org/10.1016/j.enbuild.2015.12.033.

[8] Laumbach R, Meng Q, Kipen H. What can individuals do to reduce personal health risks from air pollution? J Thorac Dis 2015;7:96–107. http://dx.doi.org/10.3978/j.issn.2072-1439.2014.12.21.

[9] European Commission. Indoor air pollution: new EU research reveals higher risks than previously thought; 2003.

[10] Steinemann A, Wargocki P, Rismanchi B. Ten questions concerning green buildings and indoor air quality. Build Environ 2017;112:351–8. http://dx.doi.org/10.1016/j.buildenv.2016.11.010.

[11] UNEP. United Nations Environment Programme; 2016. < http://staging.unep.org/sbci/AboutSBCI/Background.asp > [accessed August 11, 2017].

[12] Pasaoglu G, Fiorello D, Martino A, Scarcella G, Alemanno A, Zubaryeva A, et al. Driving and parking patterns of European car drivers - a mobility survey; 2012. http://doi.org/10.2790/7028.

[13] Brauner G, D'Haeseleer W, Gehrer W, Glaunsinger W, Krause T, Kaul H, et al. Electrical Power Vision 2040 for Europe. A document from the EUREL task force; 2012.

[14] Sartori I, Napolitano A, Voss K. Net zero energy buildings: a consistent definition framework. Energy Build 2012;48:220–32. http://dx.doi.org/10.1016/j.enbuild.2012.01.032.

[15] Parag Y, Sovacool BK. Electricity market design for the prosumer era. Nat Energy 2016;1:16032. http://dx.doi.org/10.1038/nenergy.2016.32.

[16] Miller W, Buys L. Positive-energy homes: impacts on, and implications for, ecologically sustainable urban design. Urban Des Int 2012;17:45–61. http://dx.doi.org/

10.1057/udi.2011.20.

[17] DIRECTIVE 2010/31/EU of the European Parliament and of the Council of 19 May 2010 on the energy performance of buildings. The European Parliament and the Council of the European Union; 2010.

[18] Davis Energy Group. California Zero Net Energy Buildings Cost Study; 2012.

[19] Heike Erhorn-Kluttig (INIVE/Fraunhofer Institute for Building Physics). Selected international Examples of nearly zero-energy buildings; 2015. < http://www.buildup.eu/en/node/45387 > [accessed June 12, 2017].

[20] Rolf Disch SolarArchitektur. The plus energy house; n.d. < http://plusenergiehaus.de/index.php?p=home&pid=8&L=0&host=1 > [accessed June 12, 2017].

[21] Bosch. The Energy Plus Home Sustainable living is possible today; 2011. < http://www.bosch-presse.de/pressportal/de/media/migrated_download/en/Factsheet_EnergyPlusHouse-e.pdf > [accessed June 12, 2017].

[22] Mathiesen BV. Analysis of power balancing with fuel cells & hydrogenproduction plants in Denmark. Energinet.dk; 2009.

[23] Hedegaard K, Meibom P. Wind power impacts and electricity storage - a time scale perspective. Renew Energy 2012;37:318–24. http://dx.doi.org/10.1016/j.renene.2011.06.034.

[24] Purvins A, Papaioannou IT, Debarberis L. Application of battery-based storage systems in household-demand smoothening in electricity-distribution grids. Energy Convers Manage 2013;65:272–84. http://dx.doi.org/10.1016/j.enconman.2012.07.018.

[25] Mulder FM, Weninger BMH, Middelkoop J, Ooms FGB, Schreuders H. Efficient electricity storage with a battolyser, an integrated Ni–Fe battery and electrolyser. Energy Environ Sci 2017;10:756–64. http://dx.doi.org/10.1039/C6EE02923J.

[26] Ahmadi P, Kjeang E. Realistic simulation of fuel economy and life cycle metrics for hydrogen fuel cell vehicles. Int J Energy Res 2016:714–27. http://dx.doi.org/10.1002/er.3672.

[27] Alanne K, Cao S. Zero-energy hydrogen economy (ZEH2E) for buildings and communities including personal mobility. Renew Sustain Energy Rev 2016:1–15. http://dx.doi.org/10.1016/j.rser.2016.12.098.

[28] International Energy Agency Hybrid & Electric Vehicle. Task 28 "Home Grids and V2X Technologies; 2017. < http://www.ieahev.org/tasks/home-grids-and-v2x-technologies-task-28/ > [accessed December 12, 2017].

[29] Kempton W, Letendre S. Electric vehicles as a new power source for electric utilities. Transp Res Part D Transp Environ 1997;2:157–75. 1361-9209/97.

[30] Yoldaş Y, Önen A, Muyeen SM, Vasilakos AV, Alan İ. Enhancing smart grid with microgrids: challenges and opportunities. Renew Sustain Energy Rev 2017;72:205–14. http://dx.doi.org/10.1016/j.rser.2017.01.064.

[31] Forrest KE, Tarroja B, Zhang L, Shaffer B, Samuelsen S. Charging a renewable future: the impact of electric vehicle charging intelligence on energy storage requirements to meet renewable portfolio standards. J Power Sources 2016;336:63–74. http://dx.doi.org/10.1016/j.jpowsour.2016.10.048.

[32] van der Kam M, van Sark W. Smart charging of electric vehicles with photovoltaic power and vehicle-to-grid technology in a microgrid; a case study. Appl Energy 2015;152:20–30. http://dx.doi.org/10.1016/j.apenergy.2015.04.092.

[33] Hyundai Tucson Fuel Cell SUV; n.d. < https://www.hyundaiusa.com/tucsonfuelcell/index.aspx > [accessed June 28, 2017].

[34] Toyota Mirai 2017 n.d. < https://ssl.toyota.com/mirai/fcv.html > [accessed June 28, 2017].

[35] Honda Clarity; n.d. < https://automobiles.honda.com/clarity > [accessed August 11, 2017].

[36] Mercedes-Benz GLC F-CELL in 2017 will be plug-in FCEV. Fuel Cells Bull 2016;2016:12. http://dx.doi.org/10.1016/S1464-2859(16)30222-X.

[37] Mirai External Power Supply System; n.d. < http://newsroom.toyota.co.jp/en/download/13241306 > [accessed June 28, 2017].

[38] Honda Power Exporter 9000; n.d. < http://world.honda.com/powerproducts-technology/PowerExporter9000/ > [accessed June 28, 2017].

[39] Lipman TE, Edwards JL, Kammen DM. Economic implications of net metering for stationary and motor vehicle fuel cell systems in California; 2002.

[40] Kempton W, Tomic J, Letendre S, Brooks A, Lipman T. Vehicle-to-grid power: battery, hybrid, and fuel cell vehicles as resources for distributed electric power in California. vol. IUCD-ITS-R; 2001.

[41] Williams BD, Kurani KS. Commercializing light-duty plug-in/plug-out hydrogen-fuel-cell vehicles: "Mobile Electricity" technologies and opportunities. J Power Sources 2007;166:549–66. http://dx.doi.org/10.1016/j.jpowsour.2006.12.097.

[42] Lipman TE, Edwards JL, Kammen DM. Fuel cell system economics: comparing the costs of generating power with stationary and motor vehicle PEM fuel cell systems. Energy Policy 2004;32:101–25. http://dx.doi.org/10.1016/S0140-6701(04)90146-4.

[43] Kissock JK. Combined heat and power for buildings using fuel-cell cars. In: Proc 1998 Int Sol energy Conf; 1998. p. 121–32.

[44] Alavi F, Park Lee E, van de Wouw N, De Schutter B, Lukszo Z. Fuel cell cars in a microgrid for synergies between hydrogen and electricity networks. Appl Energy 2016. http://dx.doi.org/10.1016/j.apenergy.2016.10.084.

[45] Cao S. Comparison of the energy and environmental impact by integrating a H2 vehicle and an electric vehicle into a zero-energy building. Energy Convers Manage 2016;123:153–73. http://dx.doi.org/10.1016/j.enconman.2016.06.033.

[46] Cao S, Alanne K. Technical feasibility of a hybrid on-site H2 and renewable energy system for a zero-energy building with a H2 vehicle. Appl Energy 2015;158:568–83. http://dx.doi.org/10.1016/j.apenergy.2015.08.009.

[47] Garmsiri S, Koohi-Fayegh S, Rosen MA, Smith GR. Integration of transportation energy processes with a net zero energy community using captured waste hydrogen from electrochemical plants. Int J Hydrogen Energy 2016;41:8337–46. http://dx.doi.org/10.1016/j.ijhydene.2015.11.191.

[48] Oldenbroek V, Verhoef LA, Van Wijk AJM. Fuel cell electric vehicle as a power plant: fully renewable integrated transport and energy system design and analysis for smart city areas. Int J Hydrogen Energy 2017:1–31. http://dx.doi.org/10.1016/j.ijhydene.2017.01.155.

[49] Raven R. Niche accumulation and hybridisation strategies in transition processes towards a sustainable energy system: an assessment of differences and pitfalls. Energy Policy 2007;35:2390–400. http://dx.doi.org/10.1016/j.enpol.2006.09.003.

[50] Centraal Bureau voor de Statistiek (CBS). Hernieuwbare elektriciteit; productie en vermogen; 2017. < https://opendata.cbs.nl/statline/#/CBS/nl/dataset/82610NED/table?ts=1513022584850 > [accessed December 11, 2017].

[51] WaterstofNet n.d. < http://www.waterstofnet.eu/en/realizations/hydrogen-refuelling-stations > [accessed January 22, 2017].

[52] Air liquide. Hydrogen energy. A rapidly growing solution for clean mobility; n.d. < https://www.airliquide.com/science-new-energies/hydrogen-energy > [accessed December 15, 2017].

[53] Perrin J, Steinberger-Wilckens R, Trümper SC. European hydrogen infrastructure atlas and industrial excess hydrogen analysis. PART III: Industrial distribution infrastructure; 2007.

[54] Lim TW, Ahn BK. Hyundai's FCEVs: a pathway to new possibilities. ECS Trans 2012;50:3–10. http://dx.doi.org/10.1149/05002.0003ecst.

[55] van Wijk A, Verhoef L. Our Car as Power Plant; 2014. http://doi.org/10.3233/978-1-61499-377-3-i.

[56] Oldenbroek V, Hamoen V, Alva S, Robledo C, Verhoef L, Wijk A Van. Fuel cell electric vehicle-to-grid : experimental feasibility and operational performance. In: 6th Eur PEFC electrolyser forum 2017; 2017. ISBN:978-3-905592-22-1.

[57] Prêt-à-Loger - TU Delft - Solar Decathlon Europe 2014 Project Design Introduction 2013. < https://www.youtube.com/watch?v=Oldgym0VD7g > [accessed July 3, 2017].

[58] Dobbelsteen A Van Den, Jonathan T, Kruizinga J. Prêt-à-Loger : zero-energy home with maximum living quality increase; 2015.

[59] Centraal Bureau voor de Statistiek (CBS). Energieverbruik particuliere woningen; woningtype en regio's; 2016. < http://statline.cbs.nl/StatWeb/publication/?DM=SLNL&PA=81528NED > [accessed July 17, 2017].

[60] Dutch Heat Pump Association. Heat pumps in domestic housing and demand management; 2015.

[61] van Sark WGJHM, Bosselaar L, Gerrissen P, Esmeijer K, Moraitis P, Donker M van den, et al. Update of the Dutch PV specific yield for determination of PV contribution to renewable energy production: 25% more. In: 29th Eur Photovolt Sol Energy Conf Exhib; 2013. p. 4095–7. http://doi.org/10.4229/EUPVSEC20142014-7AV.6.43.

[62] Surmeli-Anac N, Hermelink A, de Jager D, Groeneberg H. Primary energy demand of renewable energy carriers. Part 2: policy implications; 2014.

[63] Anke Esser, Frank Sensfuss. Final report. Evaluation of primary energy factor calculation options for electricity; 2016.

[64] European Parliament. Directive 2009/28/EC of the European Parliament and of the Council of 23 April 2009. Off J Eur Union 2009. http://doi.org/10.3000/17252555.L_2009.140.eng.

[65] Wehringer F, Scherberich M, Groezinger J, Boermans T, John ASJ. Overview of Member States information on NZEBs Working version of the progress report - final report. Ecofys by Order Eur Comm; 2014.

[66] Eberle U, Müller B, von Helmolt R. Fuel cell electric vehicles and hydrogen infrastructure: status 2012. Energy Environ Sci 2012;5:8780. http://dx.doi.org/10.1039/c2ee22596d.

[67] Centraal Bureau voor de Statistiek (CBS). Verkeersprestaties personenauto's; kilometers, brandstofsoort, grondgebied; 2016. < http://statline.cbs.nl/Statweb/publication/?DM=SLNL&PA=80428ned&D1=0-9&D2=a&D3=a&D4=0&D5=(l-5)-l&VW=T > [accessed April 10, 2017].

[68] Hyundai Motor Company. ix35 Fuell Cell Electric Vehicle Brochure 2014:10.

[69] International Energy Agency. Technology roadmap. Hydrogen Fuel Cells 2015. http://doi.org/10.1007/SpringerReference_7300.

[70] Eurostat. Electricity and gas prices, second half of year, 2013–15 (EUR per kWh); 2016. < http://ec.europa.eu/eurostat/statistics-explained/index.php/File:Electricity_and_gas_prices_second_half_of_year_2013-15_(EUR_per_kWh)_YB16.png > [accessed April 11, 2017].

[71] kWh price offered by Powerpeers in The Netherlands for surplus local energy production, after net metering; 2017. < https://powerpeers.nl > [accessed August 30, 2017].

[72] US Department of Energy. Fuel economy of 2016 Hyundai vehicles; 2016. < https://www.fueleconomy.gov/feg/bymake/Hyundai2016.shtml > [accessed April 11, 2017].

[73] Centraal Bureau voor de Statistiek (CBS). Consumentenprijzen; gemiddelde prijzen van consumentenartikelen vanaf 2000; 2017.

[74] Höflinger J, Hofmann P, Müller H, Limbrunner M. FCREEV a fuel cell range extended electric vehicle. MTZ Worldw 2017;5:18–23.

[75] US Department of Energy. Target explanation document: onboard hydrogen storage for light-duty fuel cell vehicles; 2015.

[76] Mwasilu F, Justo JJ, Kim EK, Do TD, Jung JW. Electric vehicles and smart grid interaction: a review on vehicle to grid and renewable energy sources integration. Renew Sustain Energy Rev 2014;34:501–16. http://dx.doi.org/10.1016/j.rser.2014.03.031.

[77] Gerla M, Lee E-K, Pau G, Lee U. Internet of vehicles: from intelligent grid to autonomous cars and vehicular clouds. IEEE World Forum Internet Things 2014;2014:241–6.

[78] Marouf M, Pollard E, Nashashibi F. Automatic parallel parking and platooning to redistribute electric vehicles in a car-sharing application. IEEE Intell Veh Symp Proc 2014. http://dx.doi.org/10.1109/IVS.2014.6856574.